Energy spectra of the hydrogen atom and the harmonic oscillator in two dimensions from Bogomolny's semiclassical transfer operator

P. Biechele,* D.A. Goodings, and J.H. Lefebvre†

Department of Physics and Astronomy, McMaster University, Hamilton, Ontario, Canada L8S 4M1

(Received 5 September 1995)

The semiclassical quantization scheme formulated by Bogomolny [E.B. Bogomolny, Nonlinearity **5**, 805 (1992); Chaos **2**, 5 (1992)], employing a suitably chosen Poincaré surface of section, has been used to calculate the energy eigenvalues of the hydrogen atom in one and two dimensions and the anisotropic harmonic oscillator in two dimensions. For the two-dimensional systems it was found to be advantageous to decompose Bogomolny's transfer operator into two "half-mapping" operators. This approach, developed by Haggerty [M.R. Haggerty, Ph.D. thesis, Massachusetts Institute of Technology, 1994 (unpublished); Phys. Rev. E **52**, 389 (1995)], leads to an analytical solution for the energy eigenvalues of the hydrogen atom. However, the energies are found to depend on the quantum number n as $(n-1/4)^{-2}$, unlike the exact quantum energies, which go as $(n-1/2)^{-2}$. An attempt to explain this one-quarter shift on the basis of the Langer-modified WKB approximation is only partly successful. For the two-dimensional harmonic oscillator, numerical calculations yield results close to the exact quantum energies.

PACS number(s): 05.45.+b, 03.20.+i, 03.65.−w

I. INTRODUCTION

Recent studies of the correspondence between classical mechanics and quantum mechanics have been mainly concerned with the following problem: Assuming one has detailed knowledge of the classical motion in a chaotic system, what is the best way of using this knowledge to obtain energy eigenvalues and eigenfunctions for the analogous quantum system? Until recently, most approaches to this "semiclassical quantization problem" were based on the well known Gutzwiller trace formula [1, 2] and the closely related dynamical ζ function [3–8]. To implement these methods, however, it is essential to have a systematic way of finding all the periodic orbits of the system, as well as their actions, periods, stability exponents, and phase indices—a difficult task for a general system.

About three years ago a different approach to semiclassical quantization was developed by Bogomolny [9, 10]. Central to his theory is a transfer operator $T(q'', q'; E)$ that is constructed from the classical trajectories connecting points q' and q'' on a suitably chosen Poincaré surface of section (PSS). In a finite approximation to the transfer operator, to be described in Sec. II, approximate energy eigenvalues of the quantum system occur as the solutions of a determinantal equation. The corresponding energy eigenfunctions may also be calculated from the appropriate semiclassical Green's function [9, 11]. Bogomolny's theory has the advantage that it does not require knowing the periodic orbits of the system. Furthermore, it does not have convergence problems, is relatively easy to implement, and, as will be seen presently, it takes account of the Heisenberg uncertainty principle in a natural way.

Bogomolny's transfer operator has been found to give excellent results for the low-lying energy eigenvalues of a variety of systems, including the quantum analogs of classically integrable systems [12, 13], of classical systems exhibiting "hard chaos" [13–15], and of classical systems exhibiting "soft chaos" or mixed behavior [13, 16, 17]. ("Hard chaos" means that there exists a positive Lyapunov exponent for almost all initial conditions; "soft chaos" or mixed behavior means that there exist both regular and chaotic trajectories in the classical phase space.) In view of these successful results, one would like to know whether the transfer operator can also be used to obtain the energy spectrum of simple systems such as the harmonic oscillator and the hydrogen atom. In this paper we use the transfer operator to obtain the energy levels of the one-dimensional and two-dimensional hydrogen atoms and the two-dimensional anisotropic harmonic oscillator. Clearly, the motivation for this work has much more to do with learning about Bogomolny's transfer operator than in finding yet another way of solving the hydrogen atom or the harmonic oscillator.

The paper is organized as follows. After a brief summary of Bogomolny's theory in Sec. II, we treat the problem of the one-dimensional H atom in Sec. III. The theory of the two-dimensional H atom is developed in Sec. IV, making use of "half-mapping operators" introduced by Haggerty [16, 17]. This leads to an analytical result for the energy eigenvalues. In Sec. V, a similar approach is applied to the two-dimensional harmonic oscillator. Finally, our results are discussed in Sec. VI.

*Present address: Fakultät für Physik, Universität Freiburg, Hermann-Herder Strasse 3, 79104 Freiburg, Germany.

†Present address: Department of Physics, Washington State University, Pullman, WA 99164-2814.

II. THE TRANSFER OPERATOR AND THE DETERMINANTAL EQUATION

In Bogomolny's theory, the transfer operator is defined with respect to a given Poincaré surface of section. Although the choice of the PSS is somewhat arbitrary, the calculations are conceptually simple if one picks a "surface" in the coordinate space that is frequently crossed by the classical paths. For a system with two freedoms, the PSS is simply a one-dimensional curve. If q' and q'' are points on this curve, one obtains the transfer operator by summing over all possible classical trajectories at energy E that cross the PSS only once in going from q' to q'' and have the normal component of the momentum in the same direction at q' and q''. The result for two freedoms is [see Ref. [9], Eq. (4.18)]

$$T(q'',q';E)=\sum_{\text{cl tr}}\frac{1}{(2\pi i\hbar)^{1/2}}\left|\frac{\partial^2 S(q'',q';E)}{\partial q''\partial q'}\right|^{1/2}\times\exp[iS(q'',q';E)/\hbar-i\nu\pi/2]. \quad (1)$$

Here $S(q'',q';E)$ is the action at energy E calculated along a classical trajectory connecting the points q' and q'' and crossing the PSS only once in between. The phase index ν is related to the number of points on the trajectory at which the semiclassical approximation is not valid.

One possible way of constructing a finite approximation to the T operator in coordinate space is to divide the classically accessible part of the PSS into N cells, the nth cell centered on q_n having width Δ_n. In terms of the transfer operator $T(q_m,q_n;E)$ from q_m in cell m to q_n in cell n, the matrix element $T_{mn}(E)$ is defined to be

$$T_{mn}(E)=T(q_m,q_n;E)(\Delta_m\Delta_n)^{1/2}. \quad (2)$$

Then the condition for an energy eigenvalue is that (see [9], Sec. 8)

$$\det[I-T(E)]=0, \quad (3)$$

where I is the unit matrix. The dimension of I and the T matrix is, of course, equal to the number of cells N on the PSS.

Bogomolny writes down a prescription for the minimum number of cells required for a reasonably good numerical calculation. Suppose one wishes to calculate semiclassical energy eigenvalues E_j up to some given energy E. The coordinate q along the PSS and its conjugate momentum p lie within an area $A(E)$ of phase space accessible to the system at energy E. It is convenient to refer to the surface defined by q and p as the *PSS in phase space*, and the term *Planck cell* will be used to denote a region of this surface having an area equal to Planck's constant h. Then the number of Planck cells on the PSS in phase space that are accessible to the system at energy E is

$$N_P(E)=A(E)/h=A(E)/(2\pi\hbar). \quad (4)$$

Bogomolny argues that the T matrix of dimension $N_P(E)$ constructed in this way will be approximately unitary. He also emphasizes that in performing numerical calculations one must choose N greater than $N_P(E)$ to number obtain good numerical accuracy. In previous calculations [13] it was found that the energy eigenvalues were obtained with good accuracy when the ratio $N/N_P(E)$ was approximately 6–10. Thus the size of the cells required at energy E is consistent with the Heisenberg uncertainty principle, since the uncertainties Δq and Δp in the end points of the trajectories are such that $\Delta q\Delta p\approx\hbar/2$.

The finite approximation leading to Eq. (3) has the effect of making the solutions for the energy eigenvalues E_j complex, though usually with small imaginary parts. The real parts can be determined by locating the minima of $|\det[I-T(E)]|$ plotted as a function of E. We shall present our calculated results for the two-dimensional harmonic oscillator in this way in Sec. V.

III. THE ONE-DIMENSIONAL HYDROGEN ATOM

In this section we construct the transfer operator for the one-dimensional hydrogen atom and obtain from it the quantum energy eigenvalues. The Hamiltonian describing the electron's motion is

$$H=\frac{p^2}{2m}-\frac{e^2}{|x|}, \quad (5)$$

where m is the mass and $-e$ is the charge of the electron, p is its linear momentum, and x is its position with respect to the nucleus of charge $+e$ fixed at the origin. If the particle has a negative energy $E=-|E|$, as shown in Fig. 1, the classical motion occurs between the points $-|x_m|$ and $|x_m|$, where $|x_m|=e^2/|E|$. For this one-dimensional motion, the Poincaré surface of section for the transfer operator is simply a point, say x_0, located somewhere between $-|x_m|$ and $|x_m|$. (In fact, the PSS might consist of a finite number of points.)

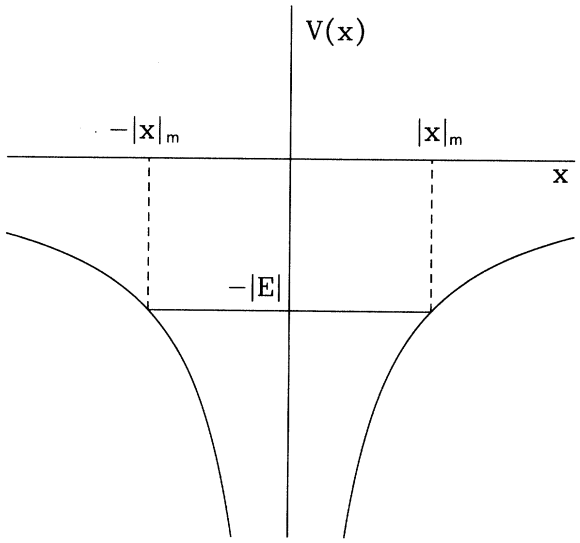

FIG. 1. Potential for the one-dimensional hydrogen atom showing the classical turning points $|x_m|$ and $-|x_m|$ corresponding to the energy E.

What are the classical trajectories that start out from x_0 in, say, the positive x direction and return to x_0 moving again in the positive x direction? One might think that if the nucleus does not act like a solid wall but only as a mathematical singularity that the classical trajectory would be the round-trip confined by the classical turning points $-|x_m|$ and $|x_m|$. However, this is not the case. A careful analysis of this one-dimensional problem in the context of celestial mechanics may be found in the treatise by Szebehely [18]. By the technique known as *regularization* (clearly described in the book by Stiefel and Scheifele [19]), in which the time variable is transformed to a new variable τ such that $d\tau = dt/|x|$, the motion of the particle is slowed down as it approaches the origin. It is then possible to show that the classical particle turns around at the nucleus and comes out again. At the end of Chap. 3 Szebehely notes that, "Already Euler [in 1765] regularized the problem of collision of two bodies moving on the same straight line." As Szebehely points out, it is illuminating to think of this motion as the limit of a two-dimensional Kepler orbit in which the eccentricity of the ellipse approaches unity. As the limit is approached, the ellipse becomes extremely narrow, the semiminor axis b and the "perihelion" distance go to zero, and the "aphelion" distance approaches the length of the major axis $2a$.

It is now clear that the PSS must consist of two points, say $|x_0|$ and $-|x_0|$, in order to treat the separate orbits along the positive and negative x axes. In both cases the action integral is

$$S(E) = 2\int_0^{|x_m|} (2m)^{1/2}(e^2/x - |E|)^{1/2}dx = \pi e^2(2m/|E|)^{\frac{1}{2}}. \tag{6}$$

(The integral is readily worked out with the help of the substitution $u^2 = |E|x/e^2$.) Also, each classical orbit has associated with it a phase index $\nu = 2$ resulting from a phase shift of $\pi/2$ occurring at each classical turning point. Furthermore, we take the prefactor in Eq. (1) to have unit modulus in order that the T matrix be unitary. This assumption is necessary because the second derivative, with respect to coordinates q' and q'' along the PSS, is undefined when the PSS consists of isolated points. Thus the T matrix corresponding to the two cells of the PSS has the form

$$T(E) = \begin{pmatrix} \exp(i\gamma)\exp[iS(E)/\hbar - i\pi] & 0 \\ 0 & \exp(i\gamma)\exp[iS(E)/\hbar - i\pi] \end{pmatrix}, \tag{7}$$

where γ is an unknown phase constant. Equation (3) then becomes

$$\{1 - \exp(i\gamma)\exp[iS(E)/\hbar - i\pi]\}^2 = 0, \tag{8}$$

the solutions of which are given by

$$S(E)/\hbar = \pm 2n\pi + \pi - \gamma, \qquad n = 0, 1, 2, \ldots. \tag{9}$$

Substituting the expression for the action from Eq. (6) we obtain

$$E_n = -\frac{me^4}{2\hbar^2(\pm n + \frac{\pi-\gamma}{2\pi})^2}. \tag{10}$$

Clearly, the energy eigenvalues depend on the phase constant γ, the value of which is not determined by the condition that the T matrix in Eq. (7) be unitary. How should it be chosen? In the usual WKB treatment of a particle moving in a one-dimensional potential $V(x)$, one obtains Eq. (9) with $\gamma = 0$. This would lead to the energy eigenvalues varying as $(n - \frac{1}{2})^{-2}$, whereas the exact solution of the Schrödinger equation for the one-dimensional hydrogen atom [20] yields Eq. (10) depending on n^{-2}. Thus the "natural choice" of $\gamma = 0$ leads to the energy eigenvalues calculated from Bogomolny's transfer operator being shifted by 1/2 from the exact energy eigenvalues. It will be recognized, however, that the choice $\gamma = \pi$, *a posteriori*, yields the correct quantum energy eigenvalues, although we do not have a good reason for making this choice.

It is interesting to note that if we had taken the classical orbit as making the round-trip between $-|x_m|$ and $+|x_m|$ instead of turning around at the nucleus, we would have obtained the wrong answer by a factor of 4. Thus the quantum system appears to "know" the correct classical orbits obtained by regularization.

IV. THE TWO-DIMENSIONAL HYDROGEN ATOM

The hydrogen atom in two dimensions presents a challenge to Bogomolny's theory because of the peculiar properties of its classical orbits. It would be natural to choose the surface of section in the plane of the motion to be a single radial line extending from the nucleus out to the maximum distance attainable at a given energy. One could then divide this line into cells having widths such that the areas of the cells in phase space are equal (as will be described in more detail later in this section). If the center of the nth cell is a distance r_n from the nucleus, the classical trajectories starting out from r_n constitute a one-parameter family of Kepler ellipses, all of which return to r_n after one revolution. As there are no other trajectories, the T matrix corresponding to the chosen cells on the PSS would be diagonal. However, for each diagonal element of T, the second derivative of the action would be infinite, because r_n is a self-conjugate point. This may be seen by examining

$$\frac{\partial^2 S(q_n'', q_n'; E)}{\partial q_n'' \partial q_n'} = -\frac{\partial p_n'}{\partial q_n''} = -\frac{1}{\partial q_n''/\partial p_n'}, \tag{11}$$

where p_n' is the radial component of the initial momentum at q_n' and q_n'' is the final position on the PSS, which

in the present situation coincides with q'_n for all the ellipses of the family of energy E. Since q''_n does not vary when the direction of the initial momentum changes (or, equivalently, when p'_n varies), $\partial q''_n/\partial p'_n = 0$ and the second derivative of the action is therefore infinite.

To circumvent this difficulty we make use of an idea employed by Haggerty [16, 17] in his studies of a smooth nonscalable potential (the Nelson potential) using Bogomolny's transfer operator. Introducing polar coordinates (r, ϕ) with the origin at the nucleus, we choose the PSS to consist of the two radial lines extending out from the nucleus in the directions $\phi = 0$ and $\phi = \pi$. We then decompose the T operator into the product $T = T_1 T_2$, in which T_1 and T_2 have the same form as in Eq. (1) but correspond to "half orbits": the operator T_1 consists of trajectories in the upper half-plane connecting different cells on the PSS and T_2 consists of trajectories in the lower half-plane connecting different cells on the PSS. With the help of the stationary phase approximation, Haggerty established the relation $T = T_1 T_2$ for the relevant operators given by Eq. (1).

The situation is illustrated in Fig. 2 in which r_1 and r_2 are the centers of cells on the lines $\phi = 0$ and $\phi = \pi$, respectively. For given energy E (which is negative) and for given r_1 and r_2, there are exactly two Kepler ellipses passing through r_1 and r_2. [A single circular path does not occur since it requires that $r_1 = r_2 = e^2/(2|E|)$, a possibility that is ruled out by the way the cells are chosen on the PSS. See Eqs. (32) to (34) below.] In order to construct the transfer operators T_1 and T_2 we require general expressions for the action, phase index, and second derivative of the action for both elliptical paths joining r_1 and r_2.

Before presenting these expressions, we first show that when r_1 and r_2 are specified, we can immediately calculate the angular momentum $L = mr^2 d\phi/dt$, which, of course, is constant. Let the two ellipses shown in Fig. 2 be written in the standard form

$$r = \frac{L^2}{me^2} \frac{1}{1 - \epsilon \cos(\phi \mp \phi_0)}, \tag{12}$$

where ϵ is the ellipticity and $\pm\phi_0$ gives the orientation of the major axis of the ellipse with respect to the line $\phi = 0$. (In writing the ellipses in this form, we are assuming that $r_1 > r_2$. The case $r_2 > r_1$ requires that the sign preceding ϵ in the denominator be changed to $+$.) Setting $\phi = 0$ in Eq. (12) we obtain for both ellipses

$$r_1 = \frac{L^2}{me^2} \frac{1}{1 - \epsilon \cos\phi_0}. \tag{13}$$

Similarly, setting $\phi = \pi$ in Eq. (12) we obtain for both ellipses,

$$r_2 = \frac{L^2}{me^2} \frac{1}{1 + \epsilon \cos\phi_0}. \tag{14}$$

Eliminating $\epsilon \cos\phi_0$ from these equations, we have

$$L^2 = 2me^2 \frac{r_1 r_2}{r_1 + r_2}. \tag{15}$$

The same result is obtained from a similar calculation for the case $r_1 < r_2$.

To obtain expressions for the actions along the two paths from r_1 to r_2, we first write

$$S(r_2, r_1; E) = \int_{r_1}^{r_2} p_r dr + \int_0^{\pi} p_\phi d\phi = \int_{r_1}^{r_2} p_r dr + L\pi, \tag{16}$$

with $p_r = \pm(2m)^{1/2}[e^2/r - |E| - L^2/(2mr^2)]^{1/2}$. Let the perihelion and aphelion distances be $r_{\min}$ and $r_{\max}$, respectively. The indefinite integral over r can be shown to be

$$\begin{aligned} S(r) &= (2m)^{1/2} \int [e^2/r - |E| - L^2/(2mr^2)]^{1/2} dr \\ &= (2m)^{1/2}[e^2 r - |E| r^2 - L^2/(2m)]^{1/2} \\ &\quad - \frac{(2m)^{1/2} e^2}{2|E|^{1/2}} \sin^{-1}[(e^2 - 2|E|r)/\alpha] \\ &\quad - L \sin^{-1}[(e^2 r - L^2/m)/(\alpha r)], \end{aligned} \tag{17}$$

where $\alpha = [e^4 - 2|E|L^2/m]^{1/2}$. Then along the path from r_1 to r_2 that passes through $r_{\max}$ we obtain

$$\begin{aligned} S_a(r_2, r_1; E) &= \int_{r_1}^{r_{\max}} |p_r| dr - \int_{r_{\max}}^{r_2} |p_r| dr + L\pi \\ &= 2S(r_{\max}) - S(r_1) - S(r_2) + L\pi \\ &= \frac{\pi e^2 (2m)^{1/2}}{2|E|^{1/2}} - S(r_1) - S(r_2). \end{aligned} \tag{18}$$

Similarly, along the path that passes through $r_{\min}$ we obtain

$$S_b(r_2, r_1; E) = \frac{\pi e^2 (2m)^{1/2}}{2|E|^{1/2}} + S(r_1) + S(r_2). \tag{19}$$

To derive an expression for the second derivative of the

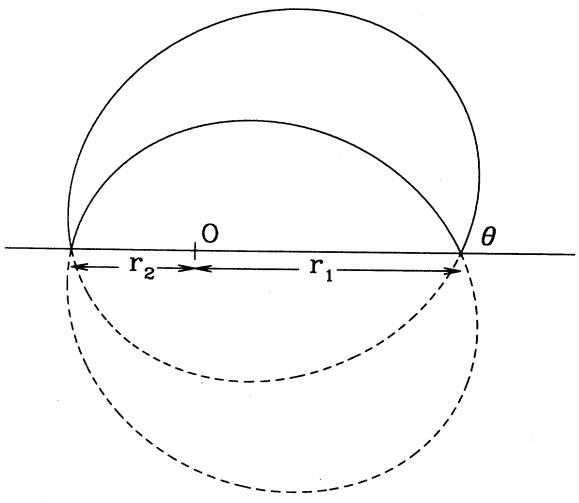

FIG. 2. Two ellipses passing through the points r_1 and r_2 on the PSS. The trajectories for T_1 are shown as solid lines, while the trajectories for T_2 are shown as the dashed lines. The angle θ is the "shooting angle" for the upper ellipse.

action in terms of $|E|$, r_1 and r_2 we first write

$$\frac{\partial^2 S(r_2,r_1;E)}{\partial r_2 \partial r_1} = -\frac{\partial p_1}{\partial r_2} = -\frac{1}{\partial r_2/\partial p_1}, \tag{20}$$

where p_1 is the radial component of the momentum at position r_1. Let θ be the angle between the tangent to the upper ellipse in Fig. 2 at r_1 and the line $\phi = 0$. Haggerty calls this the "shooting angle." From the symmetry of the two ellipses, the shooting angle of the lower ellipse is $\pi - \theta$. Since the angular momentum at $(r = r_1, \phi = 0)$ is $L = r_1 p \sin\theta = r_1 p \sin(\pi - \theta)$, where p is the magnitude of the linear momentum at $(r = r_1, \phi = 0)$, we find with the help of Eq. (15) and conservation of energy that

$$\sin^2\theta = \sin^2(\pi - \theta) = \frac{e^2 r_2}{(r_1 + r_2)(e^2 - r_1|E|)}. \tag{21}$$

Hence

$$r_2 = \frac{r_1(e^2 - r_1|E|)\sin^2\theta}{e^2\cos^2\theta + r_1|E|\sin^2\theta}. \tag{22}$$

We can now write the derivative on the right-hand side of Eq. (20) as

$$\left(\frac{\partial r_2}{\partial p_1}\right) = \left(\frac{\partial r_2}{\partial \theta}\right)\left(\frac{\partial \theta}{\partial p_1}\right) = \left(\frac{\partial r_2}{\partial \theta}\right) \Big/ \left(\frac{\partial p_1}{\partial \theta}\right). \tag{23}$$

Setting p_1 equal to $p\cos\theta$ or $p\cos(\pi - \theta)$ and carrying out the partial differentiations with respect to θ, we obtain, after a short calculation [eliminating $\sin\theta$ and $\cos\theta$ with the help of Eq. (21)],

$$\left|\frac{\partial^2 S(r_2,r_1;E)}{\partial r_2 \partial r_1}\right| = \frac{(2m)^{1/2}e^2}{2(r_1 + r_2)^{3/2}[e^2 - (r_1 + r_2)|E|]^{1/2}}. \tag{24}$$

This result applies to both trajectories in the upper half-plane in Fig. 2.

Finally, we must determine the phase index ν for each path, using the standard rule of incrementing ν by unity each time the radial component p_r changes direction at a classical turning point. Since the radial motion passes through either a maximum or a minimum while executing each trajectory from r_1 to r_2 (see Fig. 2), the phase indices are $\nu_a = \nu_b = 1$.

We can now write down the full T operator as the product of the half-mapping operators T_1 and T_2 [16, 17]. Let $T(r_2, r_1; E)$ describe the mapping from r_1 to r_2 in the upper half-plane (the solid lines in Fig. 2) and let $T(r_3, r_2; E)$ describe the mapping from r_2 to r_3 in the lower half-plane (the dashed curves in Fig. 2, but ending at a position r_3 to the right of the origin). Since r_2 is restricted to the range between 0 and $e^2/|E|$ on the part of the PSS to the left of the origin, the full T operator from r_1 to r_3 is, from Eq. (1),

$$T(r_3,r_1;E) = \int_0^{e^2/|E|} dr_2 T(r_3,r_2;E)T(r_2,r_1;E) = \frac{\exp(-i\pi)}{2\pi i\hbar}\int_0^{e^2/|E|} dr_2 \left|\frac{\partial^2 S(r_3,r_2;E)}{\partial r_3 \partial r_2}\right|^{1/2}\left|\frac{\partial^2 S(r_2,r_1;E)}{\partial r_2 \partial r_1}\right|^{1/2}$$
$$\times \{\exp[iS_a(r_3,r_2;E)/\hbar] + \exp[iS_b(r_3,r_2;E)/\hbar]\}\{\exp[iS_a(r_2,r_1;E)/\hbar] + \exp[iS_b(r_2,r_1;E)/\hbar]\}. \tag{25}$$

We see that there are four integrals, involving the following exponential factors:

$$\exp[iS_a(r_3,r_2;E)/\hbar + iS_a(r_2,r_1;E)/\hbar] = \exp\{i[S - S(r_3) - 2S(r_2) - S(r_1)]/\hbar\}, \tag{26a}$$

$$\exp[iS_a(r_3,r_2;E)/\hbar + iS_b(r_2,r_1;E)/\hbar] = \exp\{i[S - S(r_3) + S(r_1)]/\hbar\}, \tag{26b}$$

$$\exp[iS_b(r_3,r_2;E)/\hbar + iS_a(r_2,r_1;E)/\hbar] = \exp\{i[S + S(r_3) - S(r_1)]/\hbar\}, \tag{26c}$$

$$\exp[iS_b(r_3,r_2;E)/\hbar + iS_b(r_2,r_1;E)/\hbar] = \exp\{i[S + S(r_3) + 2S(r_2) + S(r_1)]/\hbar\}. \tag{26d}$$

The right-hand sides of these expressions were obtained from Eqs. (18) and (19). The constant S is defined to be

$$S = \frac{\pi e^2(2m)^{1/2}}{|E|^{1/2}}. \tag{27}$$

We now evaluate each of the integrals over r_2 in the stationary phase approximation. For the left-hand side of (26a), the phase is stationary when

$$\frac{\partial S_a(r_3,r_2;E)}{\partial r_2} + \frac{\partial S_a(r_2,r_1;E)}{\partial r_2} = 0 \tag{28}$$

or when

$$-p_r^{(a,l)}(r_2) + p_r^{(a,u)}(r_2) = 0. \tag{29}$$

Here $p_r^{(a,u)}(r_2)$ is the radial momentum component at the final point along trajectory a in the upper half-plane. Likewise $p_r^{(a,l)}(r_2)$ is the initial radial momentum component along trajectory a from r_2 to r_3 in the lower half-plane. Similar relations result when the stationary phase condition is written down for the left-hand sides of (26b)–(26d). In each case, the condition that the radial momentum components are equal implies that the trajectories in the upper and lower half-planes must join smoothly at r_2, the slope of the tangent to the curves being continuous at r_2. Figure 2 strongly suggests that this will happen only when trajectory a goes into trajectory b, or vice versa, and, in addition, r_3 coincides with r_1. The latter requirement can be easily proved analytically by adapting Eqs. (21) and (22) to the trajectories

going from r_2 to r_3 in the lower half-plane, imposing the requirement that the tangent varies smoothly across the join at r_2.

To evaluate the four integrals involving the exponentials in (26) by the stationary phase approximation, we first note that $S(r_2)$ given by Eq. (17) increases monotonically as r_2 goes from 0 to $e^2/|E|$. Thus there is no value of r_2 in this range at which the phase in (26a) or (26d) is stationary; the exponentials will oscillate rapidly as r_2 varies and the corresponding integrals may be taken to be zero. For the other integrals involving (26b) and (26c), the exponential factor is independent of r_2. Hence, assuming that $r_3 = r_1$ and making use of Eqs. (24) and (25) we obtain

$$T(r_1, r_1; E) = \frac{\exp(iS/\hbar - i\pi)}{2\pi i\hbar} \times \int_0^{(e^2/|E|-r_1)} \times \frac{(2m)^{1/2}e^2 dr_2}{(r_1+r_2)^{3/2}[e^2-(r_1+r_2)|E||]^{1/2}}. \tag{30}$$

The upper limit of this integral follows from the fact that $r_1 + r_2$ cannot exceed the length of the major axis of an ellipse of energy E, which is $e^2/|E|$. The integral is readily evaluated with the help of the substitution $x^2 = (r_1 + r_2)|E|$. The result is

$$T(r_1, r_1; E) = \frac{\exp(iS/\hbar - i\pi)}{2\pi i\hbar} 2(2m)^{1/2}(e^2/r_1 - |E|)^{1/2}. \tag{31}$$

When r_3 is different from r_1, the expressions on the right-hand side of (26b) or (26c) involve a factor $\exp\{\pm i[S(r_1) - S(r_3)]/\hbar\}$, which oscillates rapidly as either r_3 or r_1 varies. It is plausible that, when averaged over a small range of values of r_3 or r_1, such as the width of a cell on the PSS, its magnitude will be relatively small. We shall assume in what follows that $T(r_3, r_1; E) = 0$ when $r_3 \neq r_1$, an assumption that is consistent with the fact that all classical trajectories starting out from r_1 return to r_1 after one orbit.

To determine the energy eigenvalues of the system we make a finite approximation to the T operator in coordinate space, as in Eq. (2). At energy E the accessible region of phase space associated with the radial line $\phi = 0$ is shown in Fig. 3. The area enclosed by the upper and lower curves is

$$A(E) = 2(2m)^{1/2}\int_0^{e^2/(|E|)} (e^2/r - |E|)^{1/2} dr = \frac{\pi(2m)^{1/2}e^2}{|E|^{1/2}}. \tag{32}$$

From Eq. (4), the number of Planck cells at energy E is

$$N_P(E) = \frac{A(E)}{2\pi\hbar} = \frac{(2m)^{1/2}e^2}{2\hbar|E|^{1/2}}. \tag{33}$$

We now divide the PSS in phase space into $N_P(E)$ cells, each having area equal to h, as illustrated in Fig. 3.

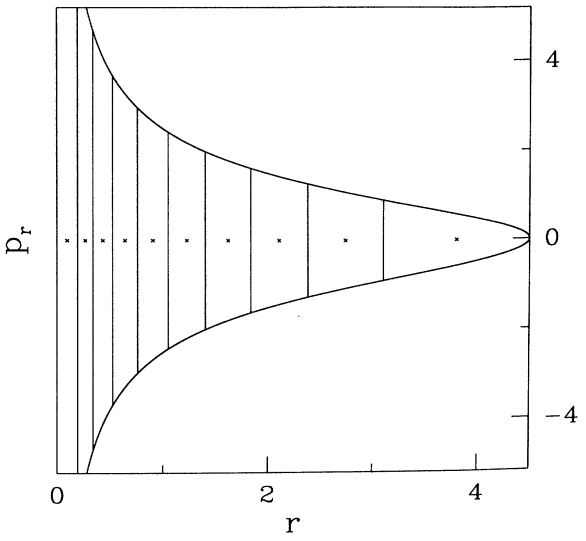

FIG. 3. PSS in phase space showing the classically accessible region on the right-hand side of the origin. The phase-space cells are of equal area.

(Other ways of choosing the cells on the PSS in phase space have not been investigated for the present problem.) The width Δ_n of the cell centered on r_n is determined by

$$2(2m)^{1/2}(e^2/r_n - |E|)^{1/2}\Delta_n = 2\pi\hbar. \tag{34}$$

From Eq. (2), the nth diagonal element of the T matrix is

$$T_{nn}(E) = T(r_n, r_n; E)\Delta_n, \tag{35}$$

which, with the help of (27), (31), and (34) simplifies to

$$T_{nn}(E) = \frac{1}{i}\exp[i\pi e^2(2m)^{1/2}/(\hbar|E|^{1/2}) - i\pi]. \tag{36}$$

Note that this does not depend on r_n. We also draw attention to the factor of $1/i = \exp(-i\pi/2)$, which is responsible for the shift of one-quarter in Eq. (38) below. Since we have argued above that the transfer operator $T(r_3, r_1; E)$ is zero when $r_3 \neq r_1$, the off-diagonal elements of the matrix $T_{mn}(E)$ are zero. Consequently, the determinantal equation for the energy eigenvalues has the simple form

$$\left\{1 - \exp[i\pi e^2(2m)^{1/2}/(\hbar|E|^{1/2}) - i3\pi/2]\right\}^{N_P(E)} = 0. \tag{37}$$

Clearly, an energy eigenvalue occurs whenever the quantity in square brackets is equal to $i2n\pi$, where $n = 0, \pm1, \pm2, \ldots$. Hence the nth energy eigenvalue is

$$E_n = -\frac{me^4}{2\hbar^2(n-\frac{1}{4})^2}, \quad n = 1, 2, \ldots. \tag{38}$$

The result in Eq. (38) is to be compared with the exact quantum energy eigenvalues for the two-dimensional

hydrogen atom:

$$E_n = -\frac{me^4}{2\hbar^2(n-\frac{1}{2})^2}, \qquad n = 1, 2, \ldots. \tag{39}$$

This may be derived by looking for a solution of the radial Schrödinger equation of the form

$$R(r) = e^{-\kappa r}\sum_{k=0}^{\infty} a_k r^k \tag{40}$$

and requiring that the series terminate at some value of k equal to n (in order to obtain a solution that does not increase exponentially with r).

How can we account for the shift of 1/4 in our result derived from Bogomolny's transfer operator? It is well known that if one treats the three-dimensional hydrogen atom in the WKB approximation, it is necessary to replace $l(l+1)$ in the radial Schrödinger equation by $(l+\frac{1}{2})^2$ in order to obtain the correct energy eigenvalues. (See, for example, Ref. [21], p. 314.) This replacement is justified by the transformation due to Langer [22], which has the effect of making the radial wave function regular at $r = 0$. For the hydrogen atom in two dimensions, if the radial wave function is written as $\psi_l(r)/r^{1/2}$, the effect of the Langer transformation is to replace $l^2 - \frac{1}{4}$ in the WKB wave function by l^2 [23]. In the Appendix we examine the possibility of accounting for the 1/4 shift in the energy eigenvalues on the basis of Bogomolny's semiclassical quantization scheme being equivalent to the Langer-modified WKB approximation. The result of this analysis is that the Langer modification to the WKB approximation leads to the 1/4 shift when $l = 0$, in agreement with our results in Eq. (38), but when $l \neq 0$, it yields the same result as the exact quantum energies, Eq. (39). Thus the 1/4 shift in *all* the energy eigenvalues is not explained by the Langer-modified WKB approximation.

Another possible explanation of the 1/4 shift in the energy eigenvalues is that it arose from the approximations involved in going from Eq. (25) to Eq. (31). However, it should be noted that the stationary phase approximation was invoked only to argue that the contributions to Eq. (25) from (26a) and (26d) may be taken to be zero for all values of r_1 and r_3 and that the contributions from (26b) and (26c) may be taken to be zero whenever $r_1 \neq r_3$. When $r_1 = r_3$, the contributions to (25) from (26b) and (26c) are given *exactly* by Eq. (31). Thus, for the crucial matrix elements given by (31), the stationary phase approximation has not been employed to work out the integral. Consequently, one cannot blame the 1/4 shift on an "extra" use of the stationary phase approximation associated with the half-mapping operators. (In fact, studying this possible explanation of the 1/4 shift, which was present in earlier numerical calculations, led us to the present analytical solution.)

V. THE TWO-DIMENSIONAL HARMONIC OSCILLATOR

The trick of decomposing the transfer operator into half-mapping operators T_1 and T_2 also provides an efficient way of finding the energy spectrum of the two-dimensional harmonic oscillator by Bogomolny's semiclassical method. Here, however, the full T operator is not diagonal in the position coordinates on the PSS and, as a result, we have not found an analytic derivation of the energy eigenvalues. Nevertheless, the use of half-mapping operators for this system is advantageous and leads to straightforward numerical calculations.

The Hamiltonian of the system is

$$H = \frac{1}{2m}(p_x^2 + p_y^2) + \frac{1}{2}m(\omega_x^2 x^2 + \omega_y^2 y^2). \tag{41}$$

It is assumed that the oscillator is anisotropic ($\omega_x \neq \omega_y$) and that $\omega_y > \omega_x$. We choose the Poincaré surface of section to be along the x axis. When the energy of the oscillator is E, the motion is restricted to the region from $x = -[2E/(m\omega_x^2)]^{1/2}$ to $x = [2E/(m\omega_x^2)]^{1/2}$. This interval is then divided into N cells (where N is even), the nth cell having its center at x_n with width Δ_n. The widths Δ_n are chosen so that the cells on the PSS in phase space have equal area. [The area of the nth phase-space cell is approximately $2\Delta_n(2mE - m^2\omega_x^2 x_n^2)^{1/2}$.]

Let us consider how to construct the operator T_1, which consists of classical trajectories connecting different cells on the PSS in the upper half-plane. Choose any two cells on the PSS and denote their centers by x_1 and x_2. In general there is at most one classical trajectory in the upper half-plane going from x_1 to x_2, as we shall see presently. For this trajectory we require expressions for the action $S(x_2, x_1; E)$, the phase index ν, and the second derivative $\partial^2 S/\partial x_1 \partial x_2$.

To find $S(x_2, x_1; E)$ we first calculate the function

$$W(x_2, x_1; T) = \int_0^T (\tfrac{1}{2}m\dot{x}^2 - \tfrac{1}{2}m\omega_x^2 x^2)dt + \int_0^T (\tfrac{1}{2}m\dot{y}^2 - \tfrac{1}{2}m\omega_y^2 y^2)dt, \tag{42}$$

with $T = \pi/\omega_y$, the time for the trajectory to go from x_1 to x_2. Setting $y(t) = \bar{y}\sin(\omega_y t)$, we find that the second integral is zero. The first integral will be evaluated from $x(t) = \bar{x}\sin(\omega_x t + \phi)$ after finding $\bar{x}$ and ϕ such that

$$x_1 = \bar{x}\sin\phi, \qquad x_2 = \bar{x}\sin(\omega_x T + \phi). \tag{43}$$

The solution is

$$\tan\phi = \frac{x_1 \sin(\omega_x T)}{x_2 - x_1\cos(\omega_x T)}, \tag{44}$$

$$\bar{x} = \frac{[x_1^2 + x_2^2 - 2x_1 x_2 \cos(\omega_x T)]^{1/2}}{\sin(\omega_x T)}. \tag{45}$$

Note that of the two possible choices for ϕ given by Eq. (44) (which differ by the angle π), we require the one that gives the correct sign for x_1, which may be positive or negative. Thus, provided that $\bar{x}$ does not exceed $[2E/(m\omega_x^2)]^{1/2}$, there is only one classical trajectory from x_1 to x_2, as stated above. It is also worth noting that because we assumed $\omega_y > \omega_x$ and since $T = \pi/\omega_y$, the denominator of Eq. (45) is positive and nonzero. Using these results we can evaluate the first integral in Eq. (42),

obtaining the familiar result [24, 25]

$$W(x_2,x_1;T)=\frac{m\omega_x}{2\sin(\omega_x T)}[(x_1^2+x_2^2)\cos(\omega_x T)-2x_1x_2]. \tag{46}$$

Finally, the action is given by

$$S(x_2,x_1;E)=W(x_2,x_1;T)+ET, \tag{47}$$

with $T=\pi/\omega_y$, and the second derivative is

$$\frac{\partial^2 S}{\partial x_1\partial x_2}=-\frac{m\omega_x}{\sin(\omega_x\pi/\omega_y)}, \tag{48}$$

which is a constant, independent of x_1 and x_2.

As in the case of the hydrogen atom in two dimensions, we take the phase index ν to be unity for the classical trajectory of a given half-mapping. The reason is that when the motion during the half-mapping is viewed in polar coordinates, one sees that the radial component passes through a single turning point.

We are now in a position to construct the $N\times N$ half-mapping matrix T_1. From Eqs. (1), (2), and (48) the matrix element for the classical trajectory from x_1 to x_2 on the PSS is

$$\langle x_2|T_1|x_1\rangle=\frac{1}{(2\pi i\hbar)^{1/2}}\left|\frac{m\omega_x}{\sin(\omega_x\pi/\omega_y)}\right|^{1/2}\times\exp[iS(x_2,x_1;E)/\hbar-i\pi/2](\Delta_1\Delta_2)^{1/2}, \tag{49}$$

with $S(x_2,x_1;E)$ given by Eqs. (46) and (47). The same expression can be used to calculate $\langle x_1|T_1|x_2\rangle$; $T_1(E)$ is a symmetric matrix.

The transfer matrix T_2 involving classical trajectories in the lower half-plane has the same form as T_1 because the harmonic oscillator potential is symmetric under reflections in the x axis. Haggerty's theorem [16, 17], $T=T_1T_2$, applied to Eq. (3), gives the following equation for the energy eigenvalues:

$$\det[(I-T_1)(I+T_1)]=0, \tag{50}$$

which is equivalent to

$$\det[I-T_1(E)]=0 \quad \text{or} \quad \det[I+T_1(E)]=0. \tag{51}$$

The first of these equations is associated with eigenfunctions that are even when $y\to -y$, while the second is associated with eigenfunctions that are odd.

In Figs. 4 and 5 we show plots of $|\det[I-T_1(\tilde{E})]|$ and $|\det[I+T_1(\tilde{E})]|$ as a function of the scaled energy $\tilde{E}$. For the calculations we chose $\omega_x=0.5$ and $\omega_y=0.9$, with the units corresponding to $m=\hbar=1$. From the exact quantum energy eigenvalues of the anisotropic harmonic oscillator

$$E_{n_xn_y}=\hbar\omega_x(n_x+\tfrac{1}{2})+\hbar\omega_y(n_y+\tfrac{1}{2}),$$

$$n_x=0,1,\ldots;\quad n_y=0,1,\ldots, \tag{52}$$

and the definition

$$\tilde{E}=\frac{E^2}{2\hbar\omega_x\hbar\omega_y}, \tag{53}$$

the corresponding scaled energy eigenvalues are readily calculated. The vertical dashed lines in Fig. 4 show the positions of the lowest 22 scaled eigenvalues $\tilde{E}_{n_xn_y}$ with n_y even. The solid curve in the figure is $|\det[I-T_1(\tilde{E})]|$ as a function of $\tilde{E}$, the matrix elements of $T_1(\tilde{E})$ having been calculated using Eqs. (46)–(49). In this calculation the dimension N of the matrix $T_1(\tilde{E})$ was initially set to be 20, but above $\tilde{E}=3$, it increased in such a way as to hold the ratio $N/N_P(E)$ approximately equal to 6. [The number of Planck cells on the phase-space surface of section (x,p_x) is $N_P(E)=E/(\hbar\omega_1)$.] The small discontinuities in the solid curve of Fig. 4 occur at energies at which N increased by 2. Thus, as $\tilde{E}$ increased from 3 to 40, N increased from 20 to 72. Figure 5 shows a similar plot of $|\det[I+T_1(\tilde{E})]|$ as a function of $\tilde{E}$. The vertical dashed lines are drawn at the positions of the exact eigenvalues $\tilde{E}_{n_xn_y}$ with n_y odd.

In both plots the minima of the solid curves are close to the exact scaled energy eigenvalues, but there are several eigenvalues for which there is no minimum in the calculated curve. [This situation is only slightly improved by increasing the ratio $N/N_P(E)$ from 6 to 10.] A partial understanding of what is happening may be obtained by examining the first eight minima in Fig. 4. With the eigenvalues labeled as (n_x,n_y) in accord with Eq. (52), these are, in order, (0,0), (1,0), (2,0), (3,0), (0,2), (4,0), (1,2), and (5,0). The deep minima near $\tilde{E}=7$ and $\tilde{E}=10$ correspond to (0,2) and (1,2), while the other minima, corresponding to $(n_x,0)$, become steadily less deep as n_x increases, disappearing completely by the time $n_x=5$. It seems that the present method of calculation is not well suited to describing the eigenstates with relatively large quantum numbers associated with the eigenfunctions on the PSS. We do not know of any other system for which Bogomolny's transfer operator has been found to fail in this way.

VI. DISCUSSION

Bogomolny's semiclassical quantization scheme has proven to be an excellent method for calculating approximate energy eigenvalues for classically chaotic systems [13–17]. In this paper we have applied it to two simple two-dimensional integrable systems. For the two-dimensional hydrogen atom, the half-mapping operators introduced by Haggerty [16, 17] provide a convenient technique for spreading out the one-parameter family of Kepler ellipses at energy E. The resulting energy eigenvalues have been found to have a one-quarter shift relative to the quantum numbers of the exact quantum energies. For states in which the angular momentum quantum number l is zero, a similar shift is found in the Langer-modified WKB approximation. However, when $l\neq 0$, the Langer modification does not lead to a shift from the exact energy eigenvalues. This means that we cannot regard Bogomolny's transfer operator as giving results entirely equivalent to the Langer-modified WKB approximation. Nor can we regard it as equiv-

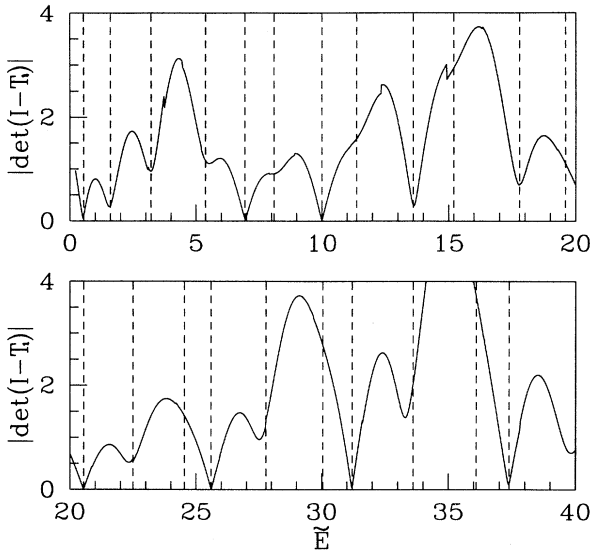

FIG. 4. Plot of $|\det[I - T_1(\tilde{E})]|$ as a function of $\tilde{E} = E^2/(2\hbar\omega_x\hbar\omega_y)$ for the two-dimensional harmonic oscillator with $\omega_x = 0.5$ and $\omega_y = 0.9$. At each energy, the dimension of the matrix $T_1(\tilde{E})$ was taken to be six times the number of Planck cells at that energy. The vertical dashed lines are located at the scaled eigenvalues $\tilde{E}_{n_x n_y}$ with n_y even.

alent to pure quantum mechanics. In previous numerical calculations employing Bogomolny's transfer operator [13, 15–17], the energy eigenvalues have not been found to be shifted from the exact quantum energies in a systematic way. The 1/4 shift found here, which was also present in our earlier numerical calculations, seems to be peculiar to the two-dimensional hydrogen atom.

With regard to the two-dimensional harmonic oscillator, our numerical calculations place the energy eigenvalues at the exact quantum energies, but fail to yield the eigenvalues corresponding to large quantum numbers associated with the PSS. We do not understand the reason for this failure.

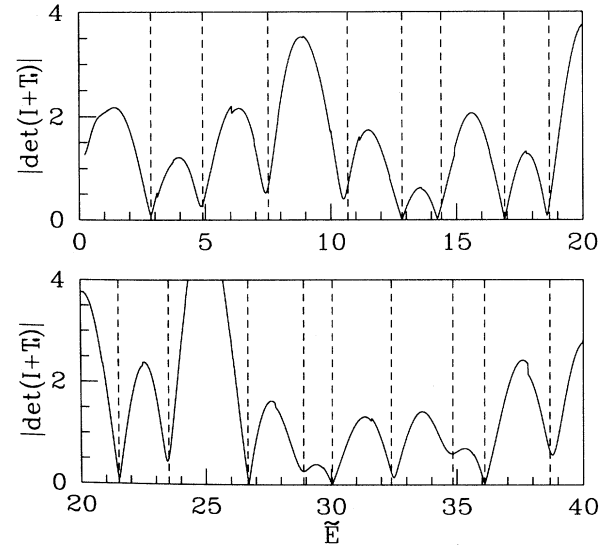

FIG. 5. Plot of $|\det[I + T_1(\tilde{E})]|$ as a function of $\tilde{E}$ calculated in the same way as in Fig. 4. The vertical dashed lines are located at the scaled eigenvalues $\tilde{E}_{n_x n_y}$ with n_y odd.

Although Bogomolny's formalism is based on a semiclassical Green's function, the precise nature of this approximation is not clear. In support of its giving exact quantum results one can point to the analytic solution obtained by Lauritzen[12] for the rectangular billiard and the calculations we have presented here for the two-dimensional harmonic oscillator. On the other hand, it has recently been shown that the wave functions for the circle billiard obtained using Bogomolny's formalism are equivalent to the Langer-modified WKB approximation [11]. In view of this "mixed" situation, it would be very interesting to know what results Bogomolny's approach yields for the three-dimensional hydrogen atom.

ACKNOWLEDGMENTS

We would like to thank Rajat Bhaduri, Michael Haggerty, Daniel Provost, Tom Szeredi, Peiqing Tong, and Niall Whelan for helpful suggestions at various stages of this work. This research was supported by the Natural Sciences and Engineering Research Council of Canada.

APPENDIX: THE LANGER-MODIFIED WKB APPROXIMATION

In this appendix we examine the ordinary WKB approximation and the Langer-modified WKB approximation, in an attempt (only partly successful) to explain the 1/4 shift in the energy eigenvalues of the two-dimensional hydrogen atom obtained by Bogomolny's transfer operator. [See Eqs. (38) and (39).] Our discussion follows closely the analysis of Berry and Ozorio de Almeida [23], who studied precisely the situation with which we are concerned—the semiclassical approximation to the radial equation for two-dimensional potentials. The analysis in Pt. 2 of Langer's paper [22], adapted to the radial equation in two dimensions, is also pertinent.

We begin with the two-dimensional Schrödinger equation containing the potential $V(r) = -e^2/r$. After separating variables and setting the angular part equal to $\exp(\pm il\phi)$ and the radial part equal to $\psi_l(r)/r^{1/2}$, we find that the wave function $\psi_l(r)$ satisfies

$$\frac{d^2\psi_l(r)}{dr^2} + \frac{1}{\epsilon^2}\left[E + \frac{e^2}{r} - \frac{\epsilon^2(l^2 - \frac{1}{4})}{r^2}\right]\psi_l(r) = 0, \tag{A1}$$

where $\epsilon^2 = \hbar^2/(2m)$ and l is the angular momentum quantum number. The standard WKB method of solving this equation leads to the approximate wave function

$$\psi_l^{\mathrm{WKB}}(r) = [Q_0(r)]^{-1/2}\exp\left(\pm i\int_{r_0}^{r} Q_0(r)dr\right), \tag{A2}$$

where

$$[Q_0(r)]^2 = \frac{1}{\epsilon^2}\left(E + \frac{e^2}{r}\right) - \frac{(l^2 - \frac{1}{4})}{r^2}. \quad \text{(A3)}$$

Here r_0 is usually chosen to be a zero of $Q_0(r)$, i.e., a classical turning point. Berry and Ozorio de Almeida show in detail that this approximation fails, for all values of l, not only at the turning points where $[Q_0(r)]^2 = 0$, but also at $r = 0$.

Langer [22] proposed a better approximate solution to equations such as (A1) by making the transformation $r = e^x$ and $\psi_l(r) = e^{x/2}u_l(r)$, the range of x being $-\infty$ to ∞. When applied to Eq. (A1) it gives

$$\frac{d^2u_l(x)}{dx^2} + [q(x)]^2 u_l(x) = 0, \quad \text{(A4)}$$

where

$$[q(x)]^2 = \frac{1}{\epsilon^2}(e^{2x}E + e^x e^2) - l^2. \quad \text{(A5)}$$

For cases in which l is *nonzero*, the WKB method applied to this equation is valid at $x = -\infty$ (which corresponds to $r = 0$). After transforming back to the variable r, we obtain the Langer-modified WKB wave function

$$\psi_l^{\text{Langer}}(r) = [Q_1(r)]^{-1/2} \exp\left(\pm i \int_{r_0}^{r} Q_1(r)dr\right), \quad \text{(A6)}$$

with

$$[Q_1(r)]^2 = \frac{1}{\epsilon^2}(E + \frac{e^2}{r}) - \frac{l^2}{r^2}. \quad \text{(A7)}$$

Comparing these equations with (A2) and (A3) we see that the effect of the Langer transformation is to replace $l^2 - \frac{1}{4}$ in $\psi_l^{\text{WKB}}(r)$ with l^2 in $\psi_l^{\text{Langer}}(r)$. When r is sufficiently small that the term $-l^2/r^2$ dominates in $[Q_1(r)]^2$, one finds from (A6) that there is a solution of the form $\psi_l^{\text{Langer}}(r) \sim r^{l+1/2}$, which is regular at $r = 0$. However, when $l = 0$ the Langer method fails completely. Berry and Ozorio de Almeida used the "method of comparison equations" to obtain a solution to Eq. (A1) for this case, which is regular at $r = 0$.

Our interest here, however, is not in obtaining accurate solutions but in finding out what the Langer-modified WKB solution of Eqs. (A4) and (A5) yields for the energy eigenvalues. We consider the cases $l \neq 0$ and $l = 0$ separately.

When $l \neq 0$ and $E < 0$, there exist inner and outer turning points of Eq. (A5) at x_1 and x_2, respectively. The function $[q(x)]^2$ can be expanded about each turning point to first order in x. The standard analysis at a linear turning point leads to the usual connection formulas for $u_l(x)$ at x_1 and x_2 [see Eq. (14) of Ref. [22] or Eq. (39) of Ref.[23]]:

$$|q(x)|^{-1/2} \exp\left(-\int_x^{x_1} |q(x)|dx\right) \longrightarrow 2|q(x)|^{-1/2} \cos\left(\int_{x_1}^{x} q(x)dx - \pi/4\right), \quad \text{(A8)}$$

$$|q(x)|^{-1/2} \exp\left(-\int_{x_2}^{x} |q(x)|dx\right) \longrightarrow 2|q(x)|^{-1/2} \cos\left(\int_{x}^{x_2} q(x)dx - \pi/4\right). \quad \text{(A9)}$$

Noting that

$$\exp(x/2)|q(x)|^{-1/2} = |Q_1(r)|^{-1/2}, \quad \text{(A10)}$$

$$\int_{x_1}^{x} q(x)dx = \int_{r_1}^{r} Q_1(r)dr, \quad \text{(A11)}$$

we can write the connection formulas for $\psi_l(r)$ as

$$|Q_1(r)|^{-1/2} \exp\left(-\int_r^{r_1} |Q_1(r)|dr\right) \longrightarrow 2|Q_1(r)|^{-1/2} \cos\left(\int_{r_1}^{r} Q_1(r)dr - \pi/4\right), \quad \text{(A12)}$$

$$|Q_1(r)|^{-1/2} \exp\left(-\int_{r_2}^{r} |Q_1(r)|dr\right) \longrightarrow 2|Q_1(r)|^{-1/2} \cos\left(\int_{r}^{r_2} Q_1(r)dr - \pi/4\right). \quad \text{(A13)}$$

In order that the solutions on the right-hand sides of these relations be the same in the region $r_1 \leq r \leq r_2$, we require that

$$\cos\left(\int_{r_1}^{r} Q_1(r)dr - \pi/4\right) = \pm \cos\left(\int_{r}^{r_2} Q_1(r)dr - \pi/4\right). \quad \text{(A14)}$$

This is satisfied if

$$\int_{r_1}^{r_2} Q_1(r)dr = (n_r - \tfrac{1}{2})\pi, \qquad n_r = 0, \pm 1, \pm 2, \ldots. \quad \text{(A15)}$$

[Equations (A14) and (A15) are the same as Berry and Ozorio de Almeida's (43) and (44).] This integral is essentially the same as the indefinite integral $S(r)$ defined in the first line of Eq. (17). With the upper and lower limits taken to be the turning points we obtain

$$\frac{\pi(2m)^{1/2}e^2}{2\hbar|E|^{1/2}} - l\pi = (n_r - \tfrac{1}{2})\pi. \quad \text{(A16)}$$

From this we find the energy eigenvalues

$$E_n = -\frac{me^4}{2\hbar^2(n - \frac{1}{2})^2}, \qquad n = 1, 2, \ldots. \quad \text{(A17)}$$

where $n = n_r + l$. These are the exact quantum energy eigenvalues as in Eq. (39). Thus the Langer-modified WKB approximation cannot explain the one-quarter shift when $l \neq 0$. [It may be noted that the ordi-

nary WKB approximation also does not account for the one-quarter shift since it would give the result in (A16) with l replaced by $(l^2 - \frac{1}{4})^{1/2}$.]

When $l = 0$ and $E < 0$, the inner turning point is $r = 0$ or $x = -\infty$. From Eq. (A7), the dominant term in $[Q_1(r)]^2$ as $r \to 0$ is $(e/\epsilon)^2/r$. Consequently, $\int_0^r Q_1(r)dr$ varies as $r^{1/2}$ for small r. In order that $\psi_0^{\text{Langer}}(r)/r^{1/2}$ be regular at $r = 0$, one must choose the linear combination of solutions of the form (A6) to be

$$\psi_0^{\text{Langer}}(r) = [Q_1(r)]^{-1/2} \sin\left(\int_0^r Q_1(r)dr\right) = [Q_1(r)]^{-1/2} \cos\left(\int_0^r Q_1(r)dr - \pi/2\right). \tag{A18}$$

[Note that if the phase angle in the sine function were nonzero, the radial wave function $\psi_0^{\text{Langer}}(r)/r^{1/2}$ would be infinite at $r = 0$.] If this cosine function is substituted on the left-hand side of Eq. (A14), the condition for matching the solutions in the interval between 0 and r_2 becomes

$$\int_0^{r_2} Q_1(r)dr = (n - \tfrac{1}{4})\pi, \quad n = 0, \pm 1, \pm 2, \ldots. \tag{A19}$$

Evaluating this integral with the help of Eq. (17) with $L = l = 0$, we obtain the energy eigenvalues

$$E_n = -\frac{me^4}{2\hbar^2(n - \frac{1}{4})^2}, \quad n = 1, 2, \ldots, \tag{A20}$$

in agreement with the result obtained using Bogomolny's method [see Eq. (38)]. Thus, only when $l = 0$ is it possible to interpret the 1/4 shift in the energy eigenvalues as due to Bogomolny's semiclassical approximation being equivalent to the Langer-modified WKB approximation.

[1] M. C. Gutzwiller, J. Math. Phys. **12**, 343 (1971).
[2] M. C. Gutzwiller, *Chaos in Classical and Quantum Mechanics* (Springer-Verlag, New York, 1990).
[3] M. V. Berry, in *Quantum Chaos and Statistical Nuclear Physics*, edited by T. H. Seligman and H. Nishioka, Lecture Notes in Physics Vol. 263 (Springer, Berlin, 1986), p. 1.
[4] A. Voros, J. Phys. A **21**, 685 (1988).
[5] M. V. Berry and J. P. Keating, J. Phys. A **23**, 4839 (1990).
[6] M. V. Berry and J. P. Keating, Proc. R. Soc. London Ser. A **437**, 151 (1992).
[7] R. Artuso, E. Aurell, and P. Cvitanović, Nonlinearity **3**, 325 (1990); **3** 361 (1990).
[8] See Chaos **2** (1) (1992), special issue on periodic orbit theory, edited by P. Cvitanović.
[9] E. B. Bogomolny, Nonlinearity **5**, 805 (1992).
[10] E. B. Bogomolny, Chaos **2**, 5 (1992).
[11] J. H. Lefebvre, Ph.D. thesis, McMaster University, 1995 (unpublished).
[12] B. Lauritzen, Chaos **2**, 409 (1992).
[13] T. Szeredi, J. H. Lefebvre, and D. A. Goodings, Nonlinearity **7**, 1463 (1994).
[14] T. Szeredi, J. H. Lefebvre, and D. A. Goodings, Phys. Rev. Lett. **71**, 2891 (1993).
[15] E. B. Bogomolny and M. Caroli, Physica D **67**, 88 (1993).
[16] M. R. Haggerty, Ph.D. thesis, Massachusetts Institute of Technology, 1994 (unpublished).
[17] M. R. Haggerty, Phys. Rev. E **52**, 389 (1995).
[18] V. G. Szebehely, *Theory of Orbits, The Restricted Problem of Three Bodies* (Academic, New York, 1967).
[19] E. L. Stiefel and G. Scheifele, *Linear and Regular Celestial Mechanics* (Springer-Verlag, New York, 1971).
[20] R. Loudon, Am. J. Phys. **27**, 649 (1959).
[21] S. Flügge, *Practical Quantum Mechanics* (Springer-Verlag, Berlin, 1974).
[22] R. E. Langer, Phys. Rev. **51**, 669 (1937).
[23] M. V. Berry and A. M. Ozorio de Almeida, J. Phys. A **6**, 1451 (1973).
[24] R. P. Feynman and A. R. Hibbs, *Quantum Mechanics and Path Integrals* (McGraw-Hill, New York, 1965), p. 63.
[25] L. S. Schulman, *Techniques and Applications of Path Integration* (Wiley, New York, 1981), p. 38.